

Fig. 11 Comparative front bourrelet normal force results for sabot models 1-7.

The analysis, being overpredictive but simple and fast, was then applied to six other sabot models, as given in Figs. 9 and 10, to examine their relative lifting capability. These sabot models and dimensions were generated by the PRODAS code.¹³ These sabots are for both the 120- and 105-mm calibers, as provided in Table 2. Note that sabot model 3 has four petals instead of the more common three-petal design. All calculations were made at Mach 4.5 and the same conditions. The resulting front bourrelet normal force on each petal model is shown in Fig. 11. Sabot models and their corresponding normal forces are provided in Table 2. These predicted forces are to be considered overestimated, possibly by a factor of about 1.6 (based on the CFD results for model 1). An actual test is recommended to be made to provide a validity for the CFD results as well. Meanwhile, the comparative results for the different sabot configurations provide some insight about the relative effectiveness of different front bourrelet designs in producing lift.

Conclusions

Aerodynamic lifting force on a closed, three-petal sabot configuration mounted on its host projectile is analyzed. The modified Newtonian theorem was used to estimate a first-order value for the lifting force on the front bourrelet (during flight in close proximity of the muzzle). CFD calculations were made, and the result suggests that the estimate obtained by the Newtonian method overpredicted the CFD value by a factor of 1.6. The present investigation provides new insight about the aerodynamic forces on the sabot, their relative magnitudes, and the role of the drag force in the sabot opening motion. The modified Newtonian method is applied to a multitude of different sabot models for 120 and 105 mm calibers, to provide comparative values for the front bourrelet lifting force.

The following conclusions are supported by the results obtained for the two-bourrelet, three-petal closed sabot configuration mounted on its host projectile. The conclusions apply to a completely closed sabot, which occurs only during the first few meters from the muzzle. First, the front bourrelet generates a lifting force (upward), but the total normal force on the petal may still be downward. Second, the drag force on the sabot petal studied was about seven times the value of the net normal force, for the configuration considered. Third, the drag force on a petal is a major contributor to the lifting up of the sabot front end, in the initial opening stage. Fourth, anatomy of the drag on the sabot is given, indicating that the front cup contributed 87% of the total drag, whereas the second contributed 11%. Note that the outring of the front cup contributes 30% of the total sabot drag. Fifth, the modified Newtonian theorem overestimated the CFD value by a factor of about 1.6 for the current sabot configuration at Mach 4.5. Use of such a method must be accompanied with that realization.

References

¹Schmidt, E. M., "Wind Tunnel Measurements of Sabot Discard Aerodynamics," U.S. Army Ballistic Research Lab., ARBRL-TR-2246, Aberdeen Proving Ground, MD, July 1980.

²Crimi, P., and Seigelman, D., "Analysis of Mechanical and Gas Dynamic Loadings During Sabot Discard for Gun-Launched Projectiles," U.S. Army Research Lab., ARBRL-CR-341, Aberdeen Proving Ground, MD, June 1977.

³Seigelman, D., Wang, J., and Crimi, P., "Computation of Sabot Discard," U.S. Army Ballistic Research Lab., ARBRL-CR-505, Aberdeen Proving Ground, MD, Feb. 1983.

⁴Nusca, M., "Computational Fluid Dynamics Application to the Aerodynamics of Symmetric Sabot Discard," AIAA Paper 90-2246, Aug. 1990.

⁵Nusca, M., "Numerical Simulation of Sabot Discard Aerodynamics," AIAA Paper 91-3255, Sept. 1991.

⁶Ferry, E., Sahu, J., and Heavey, K., "Navier-Stokes Computations of Sabot Discard Using Chimera Scheme," U.S. Army Research Lab., ARL-TR-1525, Aberdeen Proving Ground, MD, Oct. 1997.

⁷Cox, R. N., and Crabtree, L. F., *Elements of Hypersonic Aerodynamics*, English Univ. Press, London, 1965, pp. 70, 71.

⁸Lees, L., "Hypersonic Flow," *Proceeding of the 5th International Aerospace Conference*, Inst. of Aerospace Society, 1953, pp. 241-276.

⁹"Equations, Tables, and Charts for Compressible Flow," NACA Rept. 1135, Ames Aeronautical Lab., Moffett Field, CA, 1953.

¹⁰Clippinger, R. F., Giese, J. H., and Carter, W. C., "Tables of Supersonic Flow About Cone Cylinders, Part I: Surface Data," U.S. Army Ballistic Research Lab., Rept. 729, Aberdeen Proving Ground, MD, July 1950.

¹¹Sahu, J., Pressel, D., Heavey, K., and Dinavahi, S., "Parallel Numerical Computations of Projectile Flowfields," AIAA Paper 99-3138, June 1999.

¹²Edge, H. L., Sahu, J., Sturek, W. B., Pressel, D. M., Heavey, K. R., Weinacht, P., Zoltani, C. K., Clarke, J., and Behr, M., "Computational Fluid Dynamics (CFD) Computations with Zonal Navier-Stokes Flow Solver (ZNSFLOW) Common High Performance Computing Scalable Software Initiative (CHSSI) Software," U.S. Army Research Lab., ARL-TR-1987, Aberdeen Proving Ground, MD, June 1999.

¹³"PRODAS Code, Version 3.6," Arrow Tech Associates, Inc., South Burlington, VT, 1991.

R. M. Cummings
Associate Editor

Atmospheric Reentry Modeling and Simulation

R. R. Costa,* J. A. Silva,† S. F. Wu,‡
Q. P. Chu,§ and J. A. Mulder¶
Delft University of Technology,
2629 HS Delft, The Netherlands

Introduction

ATMOSPHERIC reentry presents challenges in several domains of engineering and science, being one of the principal research fields in space technology. To provide an environment to design control laws for reentry vehicles, Delft University of Technology (TU Delft) is developing a simulation tool for atmospheric reentry. The simulation tool is called general simulator for atmospheric reentry dynamics (GESARED) and was implemented in MATLAB®/SIMULINK. The simulation tool is meant to work on a personal computer. GESARED was initially developed to be the

Received 25 September 2000; revision received 15 February 2002; accepted for publication 22 February 2002. Copyright © 2002 by the American Institute of Aeronautics and Astronautics, Inc. All rights reserved. Copies of this paper may be made for personal or internal use, on condition that the copier pay the \$10.00 per-copy fee to the Copyright Clearance Center, Inc., 222 Rosewood Drive, Danvers, MA 01923; include the code 0022-4650/02 \$10.00 in correspondence with the CCC.

*Research Engineer, Faculty of Aerospace Engineering; Rodrigo.daCosta@astrium-space.com. Member AIAA.

†Graduate Student, Faculty of Aerospace Engineering; J.G.AraujodaSilva@student.TUdelft.NL.

‡Research Fellow, Faculty of Aerospace Engineering; S.F.Wu@LR.TUdelft.NL.

§Assistant Professor, Faculty of Aerospace Engineering; Q.P.Chu@LR.TUdelft.NL.

¶Professor and Chairman of the Control and Simulation Division, Faculty of Aerospace Engineering; J.A.Mulder@LR.TUdelft.NL.

design and test bed for guidance, navigation, and control (GN&C) systems for representative reentry vehicles. Its primary goal was to be the open-loop plant for reentry simulation, to be closed by a GN&C algorithm. In this Note, focus is given to the modeling of the lifting body reentry vehicle (LBRV) and the atmospheric reentry capsule (ARC), but models of other reentry vehicles are also discussed. Currently GESARED is the simulation environment used in the design of GN&C systems for the LBRV and the ARC.¹ The entry phase in Earth's atmosphere corresponds to an altitude range from 120 km to nearly zero. This phase is characterized by large variations of environmental conditions. Therefore, it is necessary to have realistic models of the environment. Because of large variations of atmospheric conditions and aerodynamic angles, the model of the vehicle's aerodynamics has major importance. The main objective is the design of control laws, and thus the models of the sensors and actuators should also be realistic, in order to obtain a reliable overall performance evaluation of the closed-loop system.

Entry Dynamics

The planetary entry motion is modeled as of six degrees of freedom (DOF), where uncoupled translational and angular motions are considered. The translational motion represents the point-mass trajectory motion. The generic kinematics and dynamics equations² that describe this motion are

$$\mathbf{F}_E = m \frac{d^2 \mathbf{r}_{cm}}{dt^2}, \quad \mathbf{V} = \frac{d\mathbf{r}_{cm}}{dt} \quad (1)$$

in which \mathbf{F}_E denotes external force, \mathbf{r}_{cm} denotes the position vector, m is the vehicle mass, and \mathbf{V} denotes the velocity vector in the inertial frame. The choice of the coordinate system is of major importance because it will influence the effectiveness of the simulation tool. The objective is to have a minimum number of constraints and maximum generality, while avoiding unduly the complexity of equations. Therefore velocity is expressed in Cartesian coordinates of north, east, and down. Position is expressed in spherical coordinates of latitude, longitude, and distance toward the Earth's center. The resulting equations of translational motion comprise three equations for velocity and three more for position,³ the external force vector components F_x , F_y , and F_z being expressed in the vertical frame. The only singularity of these equations of translational motion is when the latitude is $\pm\pi/2$. The consequence of this singularity is a constraint in the simulation tool of polar reentry trajectories. As such trajectories are very uncommon, this is not thought to limit the versatility of the tool in practice. The forces acting on the vehicle are the aerodynamic forces, the gravity force and the thrust force, resulting in the total external force \mathbf{F}_E . The aerodynamic and thrust forces are computed from both the vehicle and the environment models, given a specific flight condition. The gravity force is computed from the environment model, given the mass and the altitude of the vehicle.

The angular motion represents the rigid-body attitude motion. This motion is described by the following equations²:

$$\mathbf{M}_E = \frac{d\mathbf{H}}{dt}, \quad \boldsymbol{\omega} = \frac{d\boldsymbol{\theta}}{dt} \quad (2)$$

in which \mathbf{M}_E denotes an external moment, \mathbf{H} is the angular momentum, $\boldsymbol{\omega}$ is the angular velocity vector, and $\boldsymbol{\theta}$ is the attitude vector. Once again, it is necessary to choose the reference frames in which the attitude rates and attitude position are expressed. The angular velocities are conveniently expressed in the vehicle's body-fixed reference frame, represented by the common notation of p , q , and r . The attitude position is chosen in order to avoid singularities. If the Eulerian attitude angles of roll, pitch, and yaw are used, there will be a singularity whenever one particular angle is $\pm\pi/2$, depending on the order of rotation. This constraint might be unacceptable when dealing with planetary entries in general, and therefore a four-element quaternion is used instead. The external moments acting on the vehicle are the aerodynamic moments and the moments resulting from the activation of the thrusters. The resulting equations for angular motion³ comprise three equations for angular rates and four for the attitude quaternion, where the external moment (vector M_x , M_y , M_z) is expressed in the body-fixed reference frame.

Environment Modeling

The environment included in the simulation tool is that of the Earth. The model of the environment comprises three submodels: atmosphere, planet shape, and gravity. Two different models were used to simulate the atmosphere: the standard atmosphere 1962 and the global reference atmospheric model of 1999 (GRAM-99). The standard atmosphere of 1962 assumes the division of the atmosphere into 11 layers and linear variation of temperature with altitude.² Assuming the model of spheric Earth (an assumption used only for the atmospheric computations), the relations between pressure, density, and altitude can be extrapolated.² This model lacks accuracy, but it is simple and allows fast computations. GRAM-99, an empirical model of NASA Marshall Space Flight Center, is accurate, but because of its complexity and detail computations with this model are relatively slow. The Earth shape model is used in the computation of altitude given the distance toward the Earth's center. The model used in GESARED considers the Earth as a three-dimensional figure obtained from the rotation of an ellipse over its small axis. The Earth gravitation field model² implemented in GESARED uses the constants from the world geodetic system of 1984 (WGS-84) and the Jeffery constants until J_4 . Consequently the gravity force is dependent not only on altitude but also on latitude. The gravity model provides adequate accuracy.

Lifting Body Reentry Vehicle

The LBRV is a conceptual small reentry vehicle, based on a real-world example. The vehicle creates lift by flying at high angles of attack. The model of the spacecraft is implemented in MATLAB®/SIMULINK and consists of three models: aerodynamics, sensors, and actuators.

The available aerodynamic database is nonlinear, and it is presented in the form of look-up tables. These tables were generated merging results from computational fluid dynamics (CFD) with results from wind-tunnel tests.⁴ The aerodynamic computations are divided in two speed regions: subsonic/supersonic (Mach number ≤ 4.6) and hypersonic (Mach number ≥ 4). The aerodynamic coefficients for Mach numbers between 4 and 4.6 are computed using a "bridging" function. The resulting subsonic, supersonic, and hypersonic aerodynamic force and moment coefficients are presented depending on the control surface deflections, aerodynamic angles, angular rates, Mach number, Knudsen number, air density, and air temperature.

The LBRV has two types of sensors that are used in the reentry phase: the flush air data system (FADS) and the space-integrated global positioning system-inertial navigation system (SIGI). The FADS measures the flow velocity, angle of attack, and angle of sideslip. This sensor is representative of a state-of-the-art sensor system, developed for advanced airplanes flying in extreme conditions. The sensor consists of a parabolic probe that is mounted on the nose of the spacecraft and a flight air data computer. The probe has several holes, connected to pressure transducers. The relation between the real pressure and the measured pressure is modeled as a second-order transfer function. The relation between pressure measurements and velocity, angle of attack and angle of sideslip is highly nonlinear, and can be solved using estimation algorithms; in this case we used the least-squares algorithm. The model used for the FADS was a TUDelft model developed for the Eurofighter. The SIGI provides three navigation solutions: inertial navigation, global positioning system (GPS) navigation, and combined GPS inertial navigation. The choice of the solution used depends on the flight phase. During the blackout phase (ranging from 70 to 30 km), GPS is not available, and the inertial solution is used. In the rest of the flight, the combined solution is used. Two kinds of actuators are available during reentry: aerodynamic surfaces and reaction control system (RCS). The vehicle has two types of control surfaces, that is, flaps (left and right) and elevons (left and right). The surfaces are driven independently by using electromechanical actuators. Actuator dynamics are represented by second-order transfer functions. The RCS is a pressure-regulated nitrogen system and includes a total of 22 cold-gas thrusters. Sixteen thrusters are located in the aft portion of the spacecraft, and the other six are located in the nose of the spacecraft.

Atmospheric Reentry Capsule

The ARC is an Apollo-like shape guided unmanned capsule, whose objective is to demonstrate GN&C technology. The ARC's first flight was successfully completed in 1998 and consisted of launch, suborbital ballistic flight, reentry, and descent. For the reentry phase the modeling of the vehicle was divided in three parts: aerodynamics, sensors, and actuators.

The navigation system provides velocity and position information to the guidance and control systems to allow a landing accuracy of at least 100 km. The navigation system comprises two sensors: a strapdown inertial measuring unit (IMU) and a GPS receiver. The IMU outputs the position vector, the absolute velocity vector, and the spacecraft attitude. The GPS receiver, used to update the IMU measurements, outputs position (altitude, longitude, and latitude) and relative velocity (north, west, vertical) referenced to the WGS 84 geoid. In case of GPS failure or during blackout phase, the drag-derived altitude (DDA) is used instead. The DDA is a means of estimating the altitude by combining the measurements of aerodynamic (or nongravitational) accelerations, aerodynamic and atmospheric models. The measurement accuracy is bounded by 176 and 400 m for position, whereas velocity is bounded by 2 and 2.5 m/s. The aerodynamic database was obtained via CFD and is divided in two parts according to the flow regime: the continuum and the free molecular. To ensure a smooth transition from free molecular to continuum flow, a bridging function is used. The flow regime depends on the Knudsen number, which represents the rarefaction of the atmosphere. The aerodynamic tables only provide coefficients for the longitudinal motion. However, because the vehicle has an axis-symmetric shape the data tables can be considered valid for a total angle of attack, that is, the angle between the longitudinal body axis X_B and the velocity. Thus, from any combination of α and β three angles can be computed (one of them being the total angle of attack), with which a total lift force can be determined. This force will then be decomposed in "pure lift" ($X_B Z_B$ plane) and "side force" ($X_B Y_B$ plane). The ARC is maneuvered and stabilized by means of an RCS. The RCS for the ARC is composed of seven hydrazine thrusters positioned to generate pure moments in the three axes.

Software Validation

The validation of GESARED was performed in a stepwise approach. First, the aerodynamic, sensor, actuator, and environment models of both vehicles were separately tested, as well as the equations of motion. After successfully validating all individual GESARED blocks, we performed tests to the complete simulation tool. Thus, with the two different vehicles implemented and making use of three-DOF simulated trajectory for the LBRV and six-DOF flight trajectory for the ARC, we have data to run complementary tests not only to validate GESARED but also to allow the identification of the discrepancy sources.

The validation of GESARED with the LBRV model in the loop was performed by means of comparison between open-loop simulation results and a reference reentry trajectory. The reference trajectory was computed by the commercial validated software package for reentry trajectory optimization ASTOS,⁵ which generates an optimal drag acceleration vs velocity profile that respects the boundary constraints (maximum heat flux, dynamic pressure, and normal load). To perform the test, a simplified GESARED setup was implemented, consisting of the model of translational motion, the LBRV models, and the environment models. The inputs of the system were the initial state and the time history of the aerodynamic angles (angle of attack, sideslip angle, and bank angle) from the reference trajectory. These inputs were fed to the aerodynamic database implementation, and the resulting lift and drag forces, summed with the gravitational force obtained from the Earth model, were inserted into the equations of translational motion. The GESARED outputs (altitude, latitude, longitude, flight-path speed, azimuth and flight-path angles) were compared with the corresponding ones from the reference trajectory. The comparison was satisfactory, and thus GESARED's three-DOF translational motion model and the LBRV models (sensors, actuators, and aerodynamic database) were validated. Furthermore, the atmospheric and gravitational models were also validated.

The tests performed with the ARC models aimed to compare GESARED simulations with real flight data and, therefore, validate the simulator translational and angular motions models, the ARC aerodynamic database, and the thrusters models. Having this goal in mind and aiming to assess the origin of the mismatches, two different tests were performed. The first test setup is of six DOF, making use of the forces computed through the aerodynamic database. This simulation was performed in a purely open-loop configuration, implying that the inputs to GESARED during the entire simulation came from flight measurements (including atmospheric data, aerodynamic angles, altitude, and flight-path speed). The aerodynamic forces and moments were computed from the ARC aerodynamics, having the input from flight data fed to the aerodynamic database. These forces and moments, together with the gravity force, were inserted in the six-DOF equations of motion. In this configuration error propagation was avoided, and the atmospheric model was eliminated. This test setup enabled an evaluation of both the aerodynamic modeling and angular motion modeling. The results obtained were compared with the flight-test data, and for the attitude, the simulations and flight proved to match almost perfectly; the total velocity curve also matches with the flight measurements, whereas the flight-path angle matching is degraded. The second test setup is also of six DOF, but in this case error accumulation was not avoided as it was in the

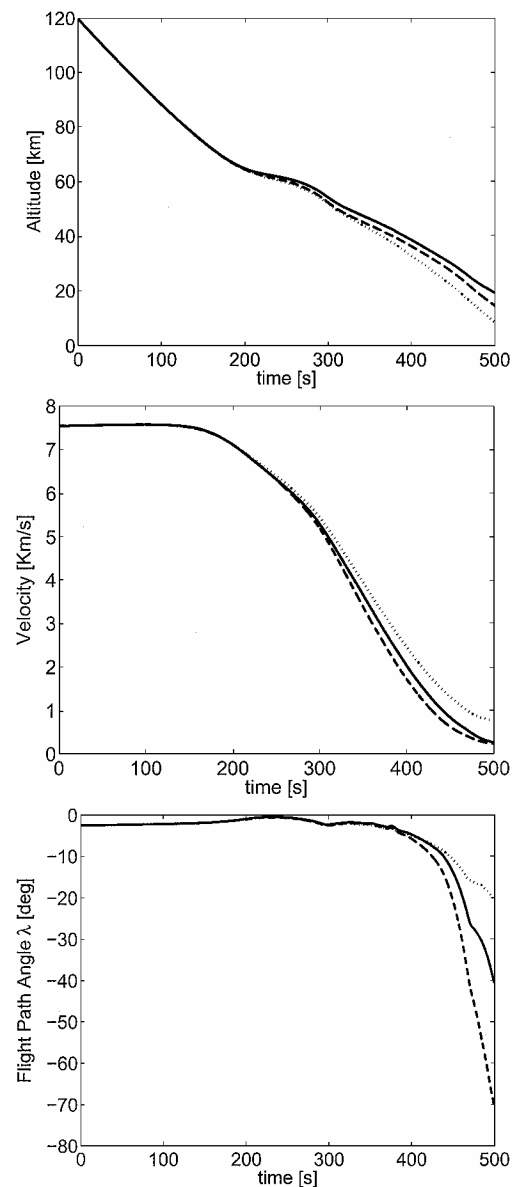


Fig. 1 ARC reentry trajectory: ····, flight data; ---, first configuration simulation; and —, second configuration simulation.

earlier test configuration. In this case the inputs of the system were the initial state at entry interface and the angular rates flight history. (There is no thruster activity data from flight.) Thus, the system state at a given instant results from the state history since the beginning of simulation. This simulator configuration is more precise because the atmospheric model is in the loop. The test allows evaluation of the ARC models and validation of GESARED. Moreover, this test can also be used for postflight analysis, and the results obtained were compared with flight data. It can be concluded that there is an increase in error, mainly resulting from error propagation. Figure 1 shows the results of both tests, compared with the real flight data. Although errors are neglectable in the beginning of the simulation, they increase toward the end, being more significant for the second test configuration. The justification for this error lies in the aerodynamic database (both simulations) and in the error accumulation (second simulation). Because in the last part of the simulation the total velocity decreases, the relative importance of forces increase, making the discrepancies between real and predicted aerodynamics more visible. These results are considered satisfactory as GESARED six-DOF simulations using attitude as reference trajectory are shown to closely match real flight measurements.

Conclusions

A new reentry simulation tool, GESARED, was implemented in the MATLAB®/SIMULINK environment. The primary objective of this simulator is to be used as a design environment of GN&C systems for reentry vehicles. As a test bed, GESARED is also designed to facilitate performance evaluations against requirements in both nominal and off-nominal conditions, allowing the entire GN&C system development process to be condensed in one tool based on a compatible, versatile, and easy-to-use environment. Moreover, GESARED is also designed to make open-loop simulations possible for model verification or postflight analysis. GESARED, more than using the potentialities of the simulation environment, has itself an open structure, allowing extensibility and model modifications. The versatility is exemplified in the set of reentry vehicles (such as the LBRV or the ARC) that can be simulated using GESARED. In addition, other entry environments (such as Mars or Titan) can be simulated.

The validation of GESARED was performed by comparing simulation results with real flight data (for the ARC) and precomputed reentry trajectory (for the LBRV). The comparison between simulation results with the LBRV models in the loop and a reference trajectory allowed the validation of the three-DOF translational motion model, the atmospheric model, the Earth model, and the LBRV models. Comparison with ARC flight data allowed wider validation, in the sense that it was possible to compare this data with the aerodynamic model of the ARC, the environment models, and the six-DOF motion models. Thus, combining the three tests performed (two with the ARC model and another with the LBRV model) it was possible to fully validate GESARED and perform the ARC postflight analysis. From the second test with the ARC model in the loop, it can be concluded that there is a neglectable mismatch between the aerodynamic model and the real vehicle. The two ARC software validation tests gave insight on the importance of error accumulation in a process as reentry, characterized by large duration and significant variation of both environment and flight conditions. Flight controller design and postflight analysis for two representative reentry vehicles were successfully conducted using the simulation tool discussed in this paper. GESARED also shows potentials in GN&C design and analysis for different reentry vehicles and missions.

References

- ¹Costa, R. R., Chu, Q. P., and Mulder, J. A., "Reentry Flight Controller Design Using Non-Linear Dynamic Inversion," *Proceedings of the Guidance, Navigation and Control Conference* [CD-ROM], AIAA, Reston, VA, 2001.
- ²Regan, F. J., and Anandkrishnan, S. M., *Dynamics of Atmospheric Re-Entry*, 1st ed., AIAA Education Series, AIAA, Washington DC, 1993, pp. 111–135.
- ³Moijj, E., *The Motion of a Vehicle in a Planetary Atmosphere*, 1st ed., Delft Univ. Press, Delft, The Netherlands, 1994, pp. 14–43.

⁴Wu, S. F., and Chu, Q. P., "The Atmospheric Re-Entry Spacecraft CRV/X-38—Aerodynamic Modeling and Analysis," ESA—European Space Technology Center, ESTEC Rept., Noordwijk, The Netherlands, July 2000.

⁵Wiegand, A., Markl, A., Well, K. H., Mehlem, K., Ortega, G., and Steinkopf, M., "AL-TOS—ESA's Trajectory Optimization Tool Applied to Re-Entry Vehicle Trajectory Design," *Proceedings of the 50th International Astronautical Federation Congress*, International Astronautical Federation, Amsterdam, 1999.

C. A. Kluever
Associate Editor

New Reliability Configuration for Large Planetary Descent Vehicles

Hüseyin Sarper* and Wolfgang J. Sauer†
University of Southern Colorado, Pueblo, Colorado 81001

Introduction

THIS Note is based on presentations^{1,2} at the past two conferences of the Mars Society. Several successive large vehicles must land in an attempt to establish the first human outpost. A single descent engine, as in the lunar module, is not under consideration because it would not provide enough reverse thrust to slow the vehicle and it would cause balance problems during landing. It was stated that, if one of the even number of engines fails while landing, the opposite engine would have to be shut off to maintain vehicle balance. The need to shut off the opposite engine presents a unique reliability problem, not readily found in the literature. Two new engine configurations are considered: a balanced four-engine (BFE) vehicle and a larger, balanced six-engine (BSE) vehicle. Figures 1 and 2 show these configurations, respectively. Both vehicles can land as long as each experiences at most one engine pair unavailability. (One engine fails, and the opposite engine is shut off.) The problem, at first, appears to be that of classic k -out-of- n (Ref. 3) reliability structure where any (random) k of the n ($k \leq n$) engines are sufficient, but this is not the case in the new problem. In fact, this problem has never been discussed in the literature before. These systems were proposed^{1,2} as theoretical future powered vehicles, but they resemble Delta Clipper (or DC-X) vehicle. Visual inspection[‡] shows four symmetrical thrust sources or engines. It appears that DC-X vehicle is relevant, and it should help to frame the state of the art. The purpose of this Note is not to perform reliability analysis of DC-X or another similar vehicle. The purpose is to provide reliability tools that can be used in making risk or probability statements on the performance of these new reliability structures, which can be used in determining the overall reliability of a large descent (or ascent) vehicle.

Problem Description and Solution

Discrete Random Variable Approach

Each engine's performance is actually a random variable. A discrete random variable is suitable if the consideration is whether an

Received 4 October 2001; revision received 8 April 2002; accepted for publication 8 April 2002. Copyright © 2002 by the American Institute of Aeronautics and Astronautics, Inc. All rights reserved. Copies of this paper may be made for personal or internal use, on condition that the copier pay the \$10.00 per-copy fee to the Copyright Clearance Center, Inc., 222 Rosewood Drive, Danvers, MA 01923; include the code 0022-4650/02 \$10.00 in correspondence with the CCC.

*Professor of Engineering and Faculty Coordinator of Colorado Space Grant Consortium at USC, 2200 Bonforte Boulevard.

†Chair of Engineering Technology and Director of Colorado Space Grant Consortium at USC, 2200 Bonforte Boulevard.

‡Data available online at <http://antwrp.gsfc.nasa.gov/apod/ap951028.html> [cited 20 March 2002].